Bayesian Compressive Sampling for Pattern Synthesis With Maximally Sparse Non-Uniform Linear Arrays

Giacomo Oliveri, *Member, IEEE*, and Andrea Massa, *Member, IEEE*

***Abstract*—A numerically-efficient technique based on the Bayesian compressive sampling (BCS) for the design of maximally-sparse linear arrays is introduced. The method is based on a probabilistic formulation of the array synthesis and it exploits a fast relevance vector machine (RVM) for the problem solution. The proposed approach allows the design of linear arrangements fitting desired power patterns with a reduced number of non-uniformly spaced active elements. The numerical validation assesses the effectiveness and computational efficiency of the proposed approach as a suitable complement to existing state-of-the-art techniques for the design of sparse arrays.**

***Index Terms*—Array synthesis, Bayesian compressive sampling (BCS), linear arrays, relevance vector machine, sparse arrays.**

I. Introduction

SYNTHESIZING antenna arrays with a minimum number of elements is a problem of high importance in those applications (e.g., satellite communications, radars, biomedical imaging, acoustics, and remote sensing) where the weight, the consumption, and the hardware/software complexity of the radiating device have a strong impact on the whole cost of the overall system [1], [2].

Non-uniform arrangements have potential advantages with respect to uniform layouts [3] such as (*a*) significantly increased resolution (i.e., decreased mainlobe width) [4], (*b*) sidelobe level control/reduction [5], and (*c*) enhanced efficiency in dealing with physically-constrained geometries (e.g., conformal architectures) [6]. However, sparsening array elements has the main drawback of reducing the control of the beam shape [1]–[7] and several approaches for the design and optimization of sparse arrangements have been proposed in the last 50 years [1]–[31] to properly address such an issue.

Dealing with beam shape control, two different problems are usually considered in the state-of-the-art literature [20]: (*I*) the minimization of the peak sidelobe level (PSL) by determining a fixed set of N element positions over an aperture and sometimes the corresponding weights; (*II*) the synthesis of a maximally-sparse array[1] radiating a desired pattern. A wide set of methods concerned with *Problem I* [2] has been investigated including random approaches [11], [15], dynamic programming [12], FIR-filter design [16], stochastic optimization methods [17], [18], [20], [24], [27]–[29], analytical techniques [22], [31], and hybrid algorithms [25], [30], as well. On the contrary, *Problem II* has received less attention and few methods have been developed [2], [3], [13], [14], [19]–[21], [23], [26]. Because of the limitations of available computers, first attempts relied on techniques requiring as few computational resources as possible such as the steepest descent method [13] and the iterative least-square technique [14]. However, those approaches have strong limitations as, for example, the need to *a-priori* know the number of active elements of the array and the aperture size [13], [14]. In order to overcome these drawbacks, a technique exploiting the simplex search was developed in [3] to find the sparsest array matching a given reference pattern. Moreover, a mixed linear programming approach was introduced in [19] with the same aim. Further developments ranging from a recursive inversion algorithm based on the Legendre transform [21], [26] up to the use of a stochastic optimizer based on the simulated annealing technique [20] or a generalized Gaussian quadrature approach [23] have been successively analyzed. More recently, *Problem II* has been solved by means of an innovative technique based on the matrix pencil method (MPM) [7]. Thanks to its efficiency, the MPM generally outperforms other synthesis techniques in terms of convergence speed and array performances [7]. Despite its effectiveness, such an approach presents some limitations as follows.

1) The locations $d_p, p = 1, \ldots, P$, of the P active elements of the array are proportional to the complex values of the non-zero roots of the generalized eigenvalue problem described in [7]. Consequently, *unphysical* complex solutions (i.e., $d_p \in \mathbb{C}$) can be generated [7] and an approximation [i.e., $d_p^{MPM} = \Re(d_p)$] is required (p. 2957—[7]) whose impact on the array performances cannot be *a-priori* estimated nor neglected;
2) No requirements on the element positions [7] can be stated. Thus, no geometrical regularity or user-desired geometric features on the synthesized array can be *a-priori* enforced;
3) The method may fail in synthesizing/matching shaped beam patterns because of the imaginary parts of d_p, $p = 1, \ldots, P$ are not usually negligible ([7, p. 2958]).

This paper is aimed at proposing an innovative, flexible, and computationally-efficient complement to the existing synthesis methods that solve *Problem II*. The method, based on the Bayesian Compressive Sampling (BCS) [32] (a robust and theoretically solid technique to produce sparse models in

Manuscript received March 19, 2010; revised June 26, 2010; accepted August 14, 2010. Date of publication December 03, 2010; date of current version February 02, 2011.

The authors are with the Department of Information Engineering and Computer Science, University of Trento, Povo 38050 Trento, Italy (e-mail: giacomo.oliveri@disi.unitn.it; andrea.massa@ing.unitn.it).

Color versions of one or more of the figures in this paper are available online at http://ieeexplore.ieee.org.

Digital Object Identifier 10.1109/TAP.2010.2096400

[1]An array with the minimum number of active elements, P, over a lattice (regular or irregular) of N positions.

regression and classification problems [33]–[35]),[2] is devoted to find the maximally-sparse array with the highest *a-posteriori* probability to match a user-defined reference pattern. Towards this end, an efficient BCS solver exploiting a fast relevance vector machine (RVM) algorithm [32], [36] is adopted.

The outline of the paper is as follows. Section II is aimed at mathematically formulating the synthesis problem and describing an algorithm for minimizing a suitable cost function that depends on the degree of sparseness of the array and the mismatch between the desired power pattern and the actual one. Section III provides a selected set of numerical results to validate the proposed approach as well as to compare its performances with state-of-the-art techniques. Finally, some conclusions are drawn (Section IV).

II. Mathematical Formulation

A. BCS Formulation

Let us consider a symmetric linear arrangement of $M = 2 \times N - \chi$ ($\chi = 0$ if an even number of elements is at hand, $\chi = 1$ otherwise) isotropic elements, $w_n \in \mathbb{R}$ being the real excitation of the n-th element pair ($n = 1, \ldots, N$). The synthesis problem is that of finding the set of array weights such that (*a*) the radiated pattern is sufficiently close to a given reference one, $E_{REF}(u)$, and (*b*) the number P of *active* (i.e., $w_n = w_{-n} = \delta_{np} w_p$, $p = 1, \ldots, P$, δ_{np} being the Kronecker function) array elements is as small as possible [3]. Towards this end, the BCS formulation is considered and similarly to [3] the following assumptions are taken into account: (*a*) the reference pattern is approximated in an arbitrary set of K angular positions $u_k, k = 1, \ldots, K$, within the visible range ($u_k \in [-1, 1]$); (*b*) the set of P active positions are constrained to a large, but finite, user-chosen set of M (i.e., $M \gg P$) candidate locations not necessarily belonging to a regular lattice. Mathematically, the problem can be formulated as follows:

Synthesis Problem—Given a set of K samples of the reference pattern, $\mathbf{E}_{REF} \in \mathbb{R}^K$, and a fidelity factor ε find the set of array weights, $\mathbf{w}$, which is maximally sparse subject to $\|\mathbf{E}_{REF} - \mathbf{E}\|^2 \leq \varepsilon$

where $\|\cdot\|$ is the ℓ_2-norm, $\mathbf{E}_{REF} \triangleq [E_{REF}(u_1), \ldots, E_{REF}(u_K)]^H$, $\mathbf{w} \triangleq [w_1, \ldots, w_N]^H$, $\mathbf{E} \triangleq [E(u_1), \ldots, E(u_K)]^H$ whose k-th entry is given by $E(u_k) = \sum_{n=1}^{N} \nu_n w_n cos[2\pi d_n u_k/\lambda]$, λ being the wavelength, d_n the distance of the n-th location from the array center ($d_1 = 0$ if $\chi = 1$), and ν_n is the Neumann's number [9] defined as $\nu_n = 2 - \chi$ if $n = 1$, and $\nu_n = 2$ otherwise.

The synthesized pattern samples $\mathbf{E}$ can be then expressed as

$$\mathbf{E} = \Psi \mathbf{w} \tag{1}$$

where $\Psi \in R^{K \times N}$ and its (k, n)-th element is given by $\psi(k, n) = \nu_n cos[2\pi d_n u_k/\lambda]$.

[2]A full treatment of BCS in terms of convergence theory, performances in benchmark and illustrative problems and relations with other classification and regression techniques can be found in [33]–[36].

To recast the problem at hand as a BCS problem, the following three steps are necessary. Let us first rewrite the ℓ_2-norm constraint ($\|\mathbf{E}_{REF} - \mathbf{E}\|^2 \leq \varepsilon$) as[3] [35]

$$\mathbf{E}_{REF} - \Psi \mathbf{w} = \mathbf{e} \tag{2}$$

where $\mathbf{e} = [e_1, \ldots, e_K]^T$ is a zero mean Gaussian error vector [32], [34], [35] with an user-defined variance σ^2 proportional to the mismatching with the reference pattern (i.e., $\sigma^2 \propto \varepsilon$). Then, let us model $\mathbf{E}_{REF}$ through a Gaussian likelihood

$$p\left(\mathbf{E}_{REF}|[\mathbf{w}, \sigma^2]\right) = \frac{1}{(2\pi\sigma^2)^{\frac{K}{2}}} \exp\left(-\frac{1}{2\sigma^2}\|\mathbf{E}_{REF} - \Psi\mathbf{w}\|^2\right) \tag{3}$$

to recast the original problem as the following linear regression one with sparseness constraints ($LRSC$)

LRSC Problem—Given $\mathbf{E}_{REF} \in \mathbb{R}^K$ find $\mathbf{w}$ and σ^2 which maximize the a-posteriori probability $p(\mathbf{w}, \sigma^2|\mathbf{E}_{REF})$ subject to the constraint that $\mathbf{w}$ is maximally-sparse.

Finally, the sparseness of $\mathbf{w}$ [34], [35] is enforced. As regards the Bayesian formulation, such a task is accomplished by introducing a sparseness prior[4] over $\mathbf{w}$ [32]. Hereinafter, the Gaussian hierarchical prior [33]–[35] is invoked

$$p(\mathbf{w}|\mathbf{a}) = \frac{\prod_{n=1}^{N} \sqrt{a_n} \exp\left(-\frac{a_n w_n^2}{2}\right)}{(2\pi)^{\frac{N}{2}}} \tag{4}$$

where $\mathbf{a} \triangleq [a_1, \ldots, a_N]$ and a_n ($n = 1, \ldots, N$) is the n-th independent hyperparameter controlling the strength of the prior over w_n [33]. To fully specify (4), the hyperpriors over $\mathbf{a}$ [i.e., $p(\mathbf{a})$] and σ^2 [i.e., $p(1/\sigma^2)$] have to be defined. The Gamma distributions are here considered [33]

$$p(\mathbf{a}) = \prod_{n=1}^{N} G(a_n|\alpha_1, \alpha_2) \tag{5}$$

and

$$p\left(\frac{1}{\sigma^2}\right) = G\left(\frac{1}{\sigma^2}\middle|\, \alpha_3, \alpha_4\right) \tag{6}$$

where $\alpha_i (i = 1, \ldots, 4)$ is the i-th *scale prior*, $G(a_n|\alpha_1, \alpha_2) \triangleq (\alpha_2^{\alpha_1} a_n^{\alpha_1 - 1} e^{-\alpha_2 a}/\Gamma(\alpha_1))$, and $\Gamma(\alpha_1) \triangleq \int_0^\infty t^{\alpha_1 - 1} e^{-t} \mathrm{d}t$ is the gamma function [33]. Thanks to (4), (5), and (6), the original synthesis problem can be finally formulated as

BCS Problem—Given $\mathbf{E}_{REF} \in \mathbb{R}^K$, find $\mathbf{w}_{BCS}$, $\mathbf{a}_{BCS}$, and σ^2_{BCS} which maximize $p([\mathbf{w}, \mathbf{a}, \sigma^2]|\mathbf{E}_{REF})$.

B. BCS Solver—The RVM Procedure

In order to determine the desired sparse solution (i.e., the unknown parameters $\mathbf{w}_{BCS}$, $\mathbf{a}_{BCS}$, and σ^2_{BCS}), the RVM method [32], [33], which theoretically guarantees to solve the

[3]It is worth pointing out that (2) and the ℓ_2-norm constraint are mathematically equivalent [35].

[4]In Bayesian inference, a *prior* represents the *a-priori* knowledge about an unknown quantity in probabilistic terms.

BCS Problem [34], is applied. Towards this end, let us consider that the posterior over all unknowns can be expressed as

$$p\left([\mathbf{w},\mathbf{a},\sigma^2]|\mathbf{E}_{REF}\right)=p\left(\mathbf{w}|[\mathbf{E}_{REF},\mathbf{a},\sigma^2]\right)p\left([\mathbf{a},\sigma^2]|\mathbf{E}_{REF}\right). \tag{7}$$

Moreover, because of (3) and (4), the posterior distribution over $\mathbf{w}$

$$p\left(\mathbf{w}|[\mathbf{E}_{REF},\mathbf{a},\sigma^2]\right)=\frac{p\left(\mathbf{E}_{REF}|[\mathbf{w},\sigma^2]\right)p(\mathbf{w}|\mathbf{a})}{p\left(\mathbf{E}_{REF}|[\mathbf{a},\sigma^2]\right)} \tag{8}$$

turns out to be equal to the following multivariate Gaussian distribution [35]

$$p\left(\mathbf{w}|[\mathbf{E}_{REF},\mathbf{a},\sigma^2]\right)=\frac{1}{(2\pi)^{\frac{N+1}{2}}\sqrt{det(\Sigma)}}\times\exp\left\{-\frac{(\mathbf{w}-\mu)^H(\Sigma)^{-1}(\mathbf{w}-\mu)}{2}\right\} \tag{9}$$

where the posterior mean and the covariance are given by $\mu=\Sigma\Psi^H\mathbf{E}_{REF}/\sigma^2$ and $\Sigma=\left((\Psi^T\Psi/\sigma^2)+A\right)^{-1}$, respectively, being $A\triangleq diag(a_1,\ldots,a_N)$.

As for the second term on the right-hand side of (7), the delta-function approximation is used [33] to model the hyperparameter posterior

$$p\left([\mathbf{a},\sigma^2]|\mathbf{E}_{REF}\right)\approx\delta\left(\mathbf{a}_{BCS},\sigma^2_{BCS}\right) \tag{10}$$

where $\mathbf{a}_{BCS}$ and σ^2_{BCS} are the most probable values, $(\mathbf{a}_{BCS},\sigma^2_{BCS})=\arg\max_{\mathbf{a},\sigma^2}\{p([\mathbf{a},\sigma^2]|\mathbf{E}_{REF})\}$, also called hyperparameter posterior *modes*. In order to determine their values, let us consider that

$$p\left([\mathbf{a},\sigma^2]|\mathbf{E}_{REF}\right)\propto p\left(\mathbf{E}_{REF}|[\mathbf{a},\sigma^2]\right)p(\mathbf{a})p(\sigma^2) \tag{11}$$

and let us assume uniform scale priors. Then, $p(\sigma^2)$ and $p(\mathbf{a})$ become constant values [33] and the maximization of (11) is equivalent to maximize the term $p(\mathbf{E}_{REF}|\mathbf{a},\sigma^2)$, whose logarithm is given by [33]

$$\begin{aligned}\mathcal{L}(\mathbf{a},\sigma^2)&\triangleq\log\left[p(\mathbf{E}_{REF}|\mathbf{a},\sigma^2)\right]\\&=-\frac{1}{2}\left[N\log 2\pi+\log|C|+\mathbf{E}^H_{REF}C^{-1}\mathbf{E}_{REF}\right]\end{aligned} \tag{12}$$

where $C=\sigma^2 I+\Psi A^{-1}\Psi^T$. It is worthwhile to point out that it is not possible to perform the maximization of the "marginal likelihood" (12) in an exact fashion, but a *type-II maximum likelihood* procedure [35] can be profitably exploited for determining an iterative re-estimation of $(\mathbf{a}_{BCS},\sigma^2_{BCS})$. Such a technique, whose Matlab implementation is available in [37], is summarized in the Appendix.

Finally, by substituting (9) and (10) in (7), one obtains that

$$\begin{aligned}&p\left([\mathbf{w},\mathbf{a},\sigma^2]|\mathbf{E}_{REF}\right)\\&\quad\approx p\left(\mathbf{w}|[\mathbf{E}_{REF},\mathbf{a},\sigma^2]\right)\rfloor_{(\mathbf{a},\sigma^2)=\left(\mathbf{a}_{BCS},\sigma^2_{BCS}\right)}.\end{aligned} \tag{13}$$

The posterior over all unknowns results a multivariate Gaussian function (9) only depending on the unknown set $\mathbf{w}$ once $(\mathbf{a}_{BCS},\sigma^2_{BCS})$ have been determined. Therefore, the value of $\mathbf{w}_{BCS}=\arg\max_{\mathbf{w}}\{p([\mathbf{w},\mathbf{a},\sigma^2]|\mathbf{E}_{REF})\}$ turns out to be equal to the posterior mean of $p(\mathbf{w}|[\mathbf{E}_{REF},\mathbf{a},\sigma^2])\rfloor_{(\mathbf{a},\sigma^2)=(\mathbf{a}_{BCS},\sigma^2_{BCS})}$ given by

$$\mathbf{w}_{BCS}=\mu\rfloor_{(\mathbf{a},\sigma^2)=\left(\mathbf{a}_{BCS},\sigma^2_{BCS}\right)}. \tag{14}$$

III. BSC Synthesis Method—Algorithmic Implementation

The algorithmic implementation of the BCS-based pattern synthesis consists of the following steps:

1) *Input Phase*—Set the reference pattern $E_{REF}(u)$, the grid of admissible locations (d_n; $n=1,\ldots,N$), the set of pattern sampling points (u_k; $k=1,\ldots,K$), the target variance σ^2 of the error term $\mathbf{e}$, and its *initial estimate* σ^2_0 for the sequential solver of the RVM algorithm (see the Appendix);
2) *Matrix Definition*—Fill the entries of the matrices $\mathbf{E}_{REF}$, Ψ, $\mathbf{e}$, and $\hat{\mathbf{E}}_{REF}=\mathbf{E}_{REF}+\mathbf{e}$;
3) *Hyperparameter Posterior Modes Estimation*—Find $(\mathbf{a}_{BCS},\sigma^2_{BCS})$ by maximizing (12) as described in the Appendix;
4) *Array Weights Estimation*—Find $\mathbf{w}_{BCS}$ by (14);
5) *Output Phase*—Return the estimated array weights, $\mathbf{w}_{BCS}$, the number of active array elements, $P_{BCS}=-\chi+2\|\mathbf{w}_{BCS}\|_0$,[5] and the corresponding hyperparameter modes $(\mathbf{a}_{BCS},\sigma^2_{BCS})$.

Starting from an user-required pattern $E_{REF}(u)$ (i.e., its sampled representation $\mathbf{E}_{REF}$), the control parameters of the synthesis process are the following variables: (*a*) $d_n, n=1,\ldots,N$; (*b*) u_k, $k=1,\ldots,K$; (*c*) σ^2, and (*d*) σ^2_0. Consequently, it is possible to synthesize arbitrary reference patterns specifying the pattern matching accuracy (*c*) and the sequential solver initialization (*d*). Moreover, the BCS method allows one to enforce pattern constraints within the whole or in a subset of the visible range (*b*) as well as to set suitable geometrical features of the array arrangement (*a*).

IV. Numerical Analysis and Assessment

This section is devoted to numerically assess potentialities and limitations of the proposed BCS approach for the design of sparse linear arrays. The numerical analysis is carried out by considering a set of representative/benchmark reference patterns to evaluate the effectiveness and reliability of the BCS in approximating a user-desired pattern. In order to evaluate the "degree of optimality" of the array designs, the following metrics and pattern descriptors are used: the matching error ε defined as[6]

$$\xi\triangleq\frac{\int_0^1\left|E_{REF}(u)-E(u)\right|^2\mathrm{d}u}{\int_0^1\left|E_{REF}(u)\right|^2\mathrm{d}u}, \tag{15}$$

the aperture length L, the mean inter-element spacing $\Delta L=L/P-1$, and the minimum spacing $\Delta L_{min}=min_{p=1,\ldots,P-1}\{|d_{p+1}-d_p|\}$.

[5]In this paper $\|\mathbf{x}\|_0$ is the ℓ_0-norm of $\mathbf{x}$ (i.e., the number of non-zero elements of $\mathbf{x}$).

[6]Only $u\in[0,1]$ is considered in the definition of ξ for symmetry reasons.

A. *BCS Sensitivity Analysis*

As a first numerical experiment, the synthesis of a non-uniform array matching a Dolph-Chebyshev pattern [2] is considered. A broadside Dolph-Chebyshev pattern with $L = 9.5\lambda$ and $PSL = -20$ [dB] is assumed as reference. Let us notice that such a pattern can be synthesized through a uniform array with $P_{UNI} = 20(\lambda/2)$-spaced elements. The BCS synthesis has been carried out by sampling $E_{REF}(u)$ at K points ($u_k \in [0,1]$, $u_k = (k-1)/(K-1)$, $k = 1,\ldots,K$) and assuming the following grid of admissible locations

$$d_n = \frac{L(n-1)}{2(N-1)}, \quad n = 1,\ldots,N. \tag{16}$$

Fig. 1(a) describes the BCS results by reporting the matching error ξ versus the number of active elements P_{BCS} for different values of the control parameters: $K = \{5,\ldots,25\}$, $\sigma^2 \in [10^{-5},1]$, $\sigma_0^2 \in [10^{-5},1]$, and $N \in [5, 5\times 10^4]$. The Pareto front of the solution set in the plane (ξ, P_{BCS}) is indicated, as well. As it can be observed, different BCS trade-off solutions are obtained with accuracy and element number in the range $\xi \in [10^{-6},2]$ and $P_{BCS} \in [5,20]$, respectively. By comparing the patterns related to three representative points of the Pareto front (i.e., $P_{BCS} = \{8,14,20\}$) with the reference one [Fig. 1(b)], it turns out that the solution with $P_{BCS} = 8$ elements provides a very poor matching ($\xi = 2.91\times 10^{-1}$), while a reliable reconstruction ($\xi = 0.99\times 10^{-4}$) is yielded choosing the solution having $P_{BCS} = 14$ [Fig. 1(b)] with a non-negligible saving of array elements with respect to the $\lambda/2$-spaced uniform array (i.e., $P_{BCS}/P_{UNI} = 0.7$). As a general by-product, it results that a value of the accuracy index around the threshold $\xi = 10^{-4}$ identifies an optimal trade-off BCS solution, whereas lower ξ values usually require more radiating elements [$P_{BCS} = 20$, $\xi = 2.03\times 10^{-6}$—Fig. 1(b)] without significant/relevant improvements in the matching of the reference pattern. As regards the resulting layouts, it is worth pointing out that the optimal BCS array ($P_{BCS} = 14$) has an aperture and an excitation displacement [Fig. 1(c)] close to those of the uniform array. This proves the effective non-uniform sampling of the ideal current distribution affording $E_{REF}(u)$. Otherwise, different apertures [e.g., $L_{BCS}\rfloor_{P=8} = 6.2\lambda$ vs. $L_{BCS}\rfloor_{P=14} = 9.5\lambda$] and weights [Fig. 1(c)] are synthesized in correspondence with greater values of ξ. As for the element arrangement, a positive feature of the BCS arrays is the enlarged inter-element spacing with respect to the corresponding uniform array [Fig. 1(c)] despite the closely-spaced admissible locations [(16)].

In order to provide a deeper understanding about the sensitivity of the BCS performances on the control parameters, Figs. 2 and 3 summarize the results of a comprehensive numerical analysis. More specifically, the matching error has been evaluated as a function of K, or σ_0^2, or σ^2, or N by setting the other parameters to the values used to obtain the optimal trade-off with $P_{BCS} = 14$ (i.e., $K = 15$, $\sigma^2 = 10^{-2}$, $\sigma_0^2 = 2.0\times 10^{-3}$, $N = 501$). For completeness, the behavior of P_{BCS} has been reported, as well. As expected [Fig. 2(a)], the pattern matching improves as the number of samples K of $E_{REF}(u)$ increases. However, ξ does not further decreases beyond a threshold value ($K = 15$) slightly above the Nyquist

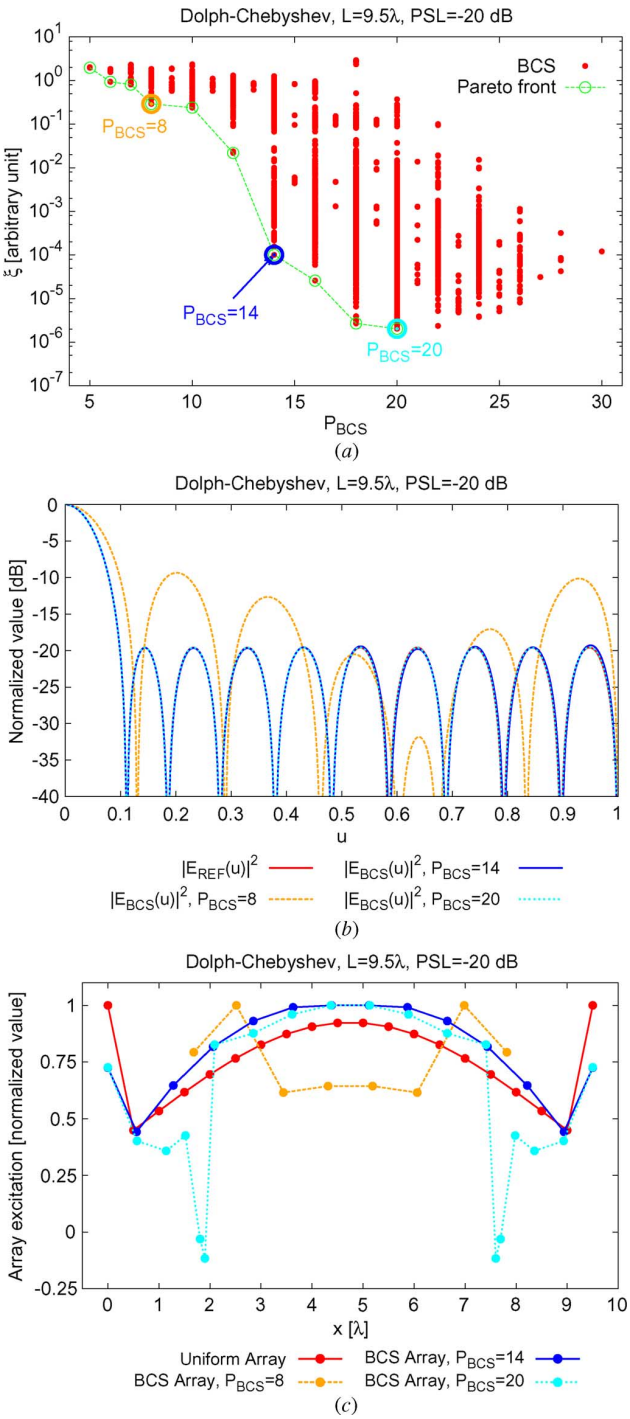

Fig. 1. *BCS Sensitivity Analysis* (*Dolph-Chebyshev*: $L = 9.5\lambda$, $PSL = -20$ dB)—Plot of the representative points of a set of BCS solutions in the (ξ, P_{BCS}) plane (*a*). Power patterns (*b*) and corresponding layouts (*c*) of the reference and of a set of representative BCS arrays.

threshold ($K_{Nyquist} = 11$) even though the corresponding number of array elements P_{BCS} still grows. A sampling value K between $K_{Nyquist}$ and $1.5K_{Nyquist}$ turns out to be a reliable choice as confirmed by the behaviour of the plots of $|E_{BCS}(u) - E_{MPM}(u)|^2$ for $K = \{7,15,24\}$ [Fig. 3(a)], as well. Indeed, the lowest value of K gives the poorest fitting [$\xi\rfloor_{K=7} = 0.91$—Fig. 3(a)], while satisfactory reconstructions are obtained when $K > K_{Nyquist}$ ($\xi\rfloor_{K=15} = 0.99\times 10^{-4}$). A

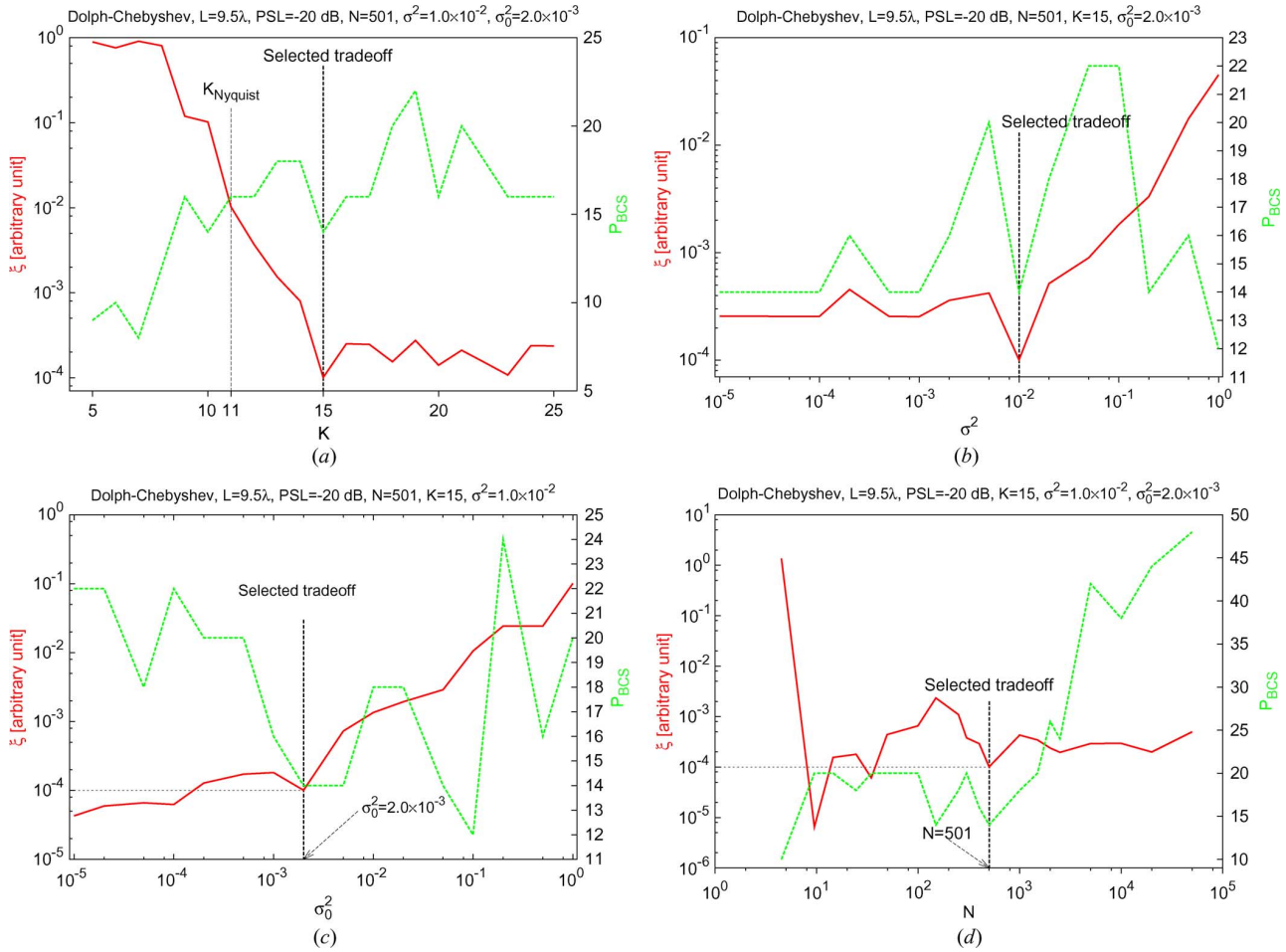

Fig. 2. *BCS Sensitivity Analysis* (*Dolph-Chebyshev*: $L = 9.5\lambda$, $PSL = -20$ dB)—Behaviours of ξ and P_{BCS} versus (*a*) K, (*b*) σ^2, (*c*) σ_0^2, and (*d*) N.

further increment of K only marginally enhances the accuracy $[\xi\rfloor_{K=24} = 0.98 \times 10^{-4}$—Fig. 3(a)].

Concerning the sensitivity to σ^2, the integral error has small variations for $\sigma^2 < 10^{-2}$, while it sharply increases afterwards [Fig. 2(b)] as pointed out by the plots of $|E_{BCS}(u) - E_{REF}(u)|^2$ in correspondence with a set of representative values of of σ^2 (i.e., $\sigma^2 = \{10^{-5}, 10^{-2}, 1\}$) [Fig. 3(b)]. More sparse arrays are synthesized in correspondence with larger values of σ^2 at the expense of higher ξ values [Fig. 2(b)]. Good tradeoffs between accuracy and element reduction then arise by setting $\sigma^2 \in [10^{-3}, 10^{-1}]$. Such an outcome indicates that the BCS performances are significantly less sensitive to σ^2 than to K. As a matter of fact, a reduction of ξ of about one order in magnitude requires a variation of K of about 10–20% [Fig. 2(a)], while the same effect holds true for a variation of σ^2 of more than two orders in magnitude [Fig. 2(b)]. Similar deductions can be drawn from the behaviour of the integral error versus σ_0^2. Moreover, the matching error increases almost monotonically with σ_0^2, whereas low P_{BCS} values are obtained within the range $\sigma_0^2 \in [5.0 \times 10^{-4}, 5.0 \times 10^{-2}]$ [Fig. 2(c)]. Such a range can be also assumed as reference guideline since smaller σ_0^2 values only marginally improve the matching accuracy [$\sigma_0^2 = 10^{-5}$, $\xi = 4.29 \times 10^{-5}$—Fig. 3(c)], while higher values do not allow reliable syntheses [$\sigma_0^2 = 1$, $\xi = 0.1$—Fig. 3(c)].

Finally, the plots in Fig. 2(d) are concerned with the sensitivity of the BCS on N. By analyzing the behaviour of P_{BCS}, it comes out that great care must be exercised on the choice of N to obtain a sparse array matching with a good accuracy the reference one. A good receipt coming also from other heuristic analyses suggests to choose $N \in [5 \times (L/\lambda); 100 \times (L/\lambda)]$.

B. BCS Assessment—Synthesis of Broadside Patterns

The second set of experiments is aimed at assessing in a more exhaustive fashion the performances of the BCS when dealing with broadside patterns. More specifically, Dolph-Chebyshev reference patterns with $L \in \{9.5\lambda, 14.5\lambda, 19.5\lambda\}$ and $PSL \in \{-20, -30, -40\}$ [dB] have been used and the Pareto fronts of the BCS solutions are shown in Fig. 4(a). As expected, wider apertures require more elements to reach the accuracy threshold $\xi = 10^{-4}$ (e.g., $P_{BCS}\rfloor_{L/\lambda=9.5} = 14$, $P_{BCS}\rfloor_{L/\lambda=14.5} = 20$, and $P_{BCS}\rfloor_{L/\lambda=19.5} = 36$). On the contrary, P_{BCS} does not generally change when varying the peak sidelobe level (e.g., $P_{BCS}\rfloor_{PSL=-20\text{ dB}} = P_{BCS}\rfloor_{PSL=-30\ dB} = P_{BCS}\rfloor_{PSL=-40\text{ dB}} = 26$). The BCS method allows a saving of about 30–35% of the array elements with respect to the corresponding uniformly $\lambda/2$-spaced array still keeping a very accurate pattern matching (i.e., $\xi < 10^{-4}$) [Table I]. This implies an increasing of the average inter-element distance $(\Delta L/(\lambda/2) \in [1.46, 1.56])$

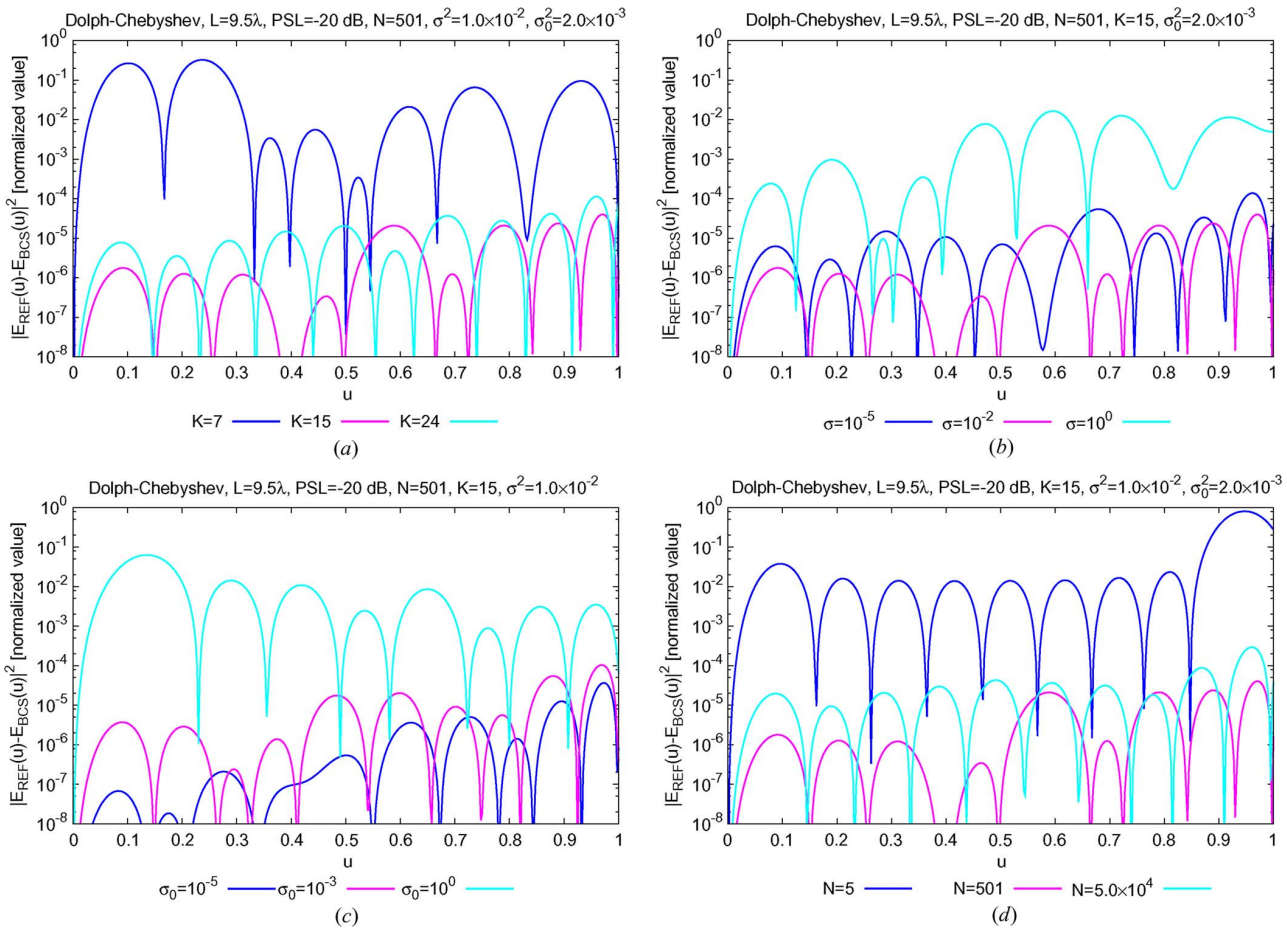

Fig. 3. *BCS Sensitivity Analysis* (*Dolph-Chebyshev*: $L = 9.5\lambda$, $PSL = -20$ dB)—Plots of $|E_{REF}(u) - E_{BCS}(u)|^2$ of representative BCS solutions computed at different values of (*a*) K, (*b*) σ^2, (*c*) σ_0^2, and (*d*) N.

and, usually, of the minimum spacing between adjacent elements ($\Delta L_{\min}/(\lambda/2) \in [1.25, 1.56]$ except for the case with $L = 19.5\lambda$ and $PSL = -30$ [dB]). However, it is worth observing that the array element saving does not yield a significant directivity reduction ($D_{BCS}/D_{UNI} \in [0.997, 1]$—Table I). Despite the lower number of elements, the directivity of the resulting sparse array is very close to that of the corresponding fully-populated arrangement thanks to the BCS ability to match a reference pattern with a high accuracy. Therefore and unlike previous array thinning techniques, no specific constraints (e.g., on the maximum percentage of antenna elements that can be thinned from an array) have to be enforced to guarantee a good directivity.

On the other hand, the array aperture only slightly reduces (e.g., $L_{BCS}/L_{UNI} = 0.995$ when $L = 19.5\lambda$ and $PSL = -30$ [dB]) since it controls the mainlobe pattern matching.

As far as the "shape" of the BCS Pareto front is concerned [Fig. 4(a)], the plot of the matching error shows a step-like behaviour whatever the array aperture and PSL conditions. Moreover, it exists a threshold value of P_{BCS} below which the BCS cannot provide an accurate matching for a given $E_{REF}(u)$. For example, the case $L = 19.5\lambda - PSL = -30$ [dB] shows that ξ decreases of more than two orders in magnitude passing from $P_{BCS} = 24$ to $P_{BCS} = 26$. This is visually pointed out in Fig. 4(c) where the plots of $|E_{BCS}(u)|^2$ for $P_{BCS} = \{24, 26\}$ are compared to the reference pattern.

Such a behaviour is further confirmed by the results in Fig. 4(b) where Taylor patterns [1] with transition index $T = 6$ and different sizes (i.e., $L \in \{9.5\lambda, 14.5\lambda, 19.5\lambda\}$) and PSLs (i.e., $PSL \in \{-20, -30, -40\}$ [dB]) are taken into account. Also in this case, a small variation of P_{BCS} ($P_{BCS} = 24 \rightarrow 26$) leads to a significant improvement of the reconstruction accuracy ($\xi\rfloor_{P_{BCS}=24} = 8.11\times10^{-3} \rightarrow \xi\rfloor_{P_{BCS}=26} = 3.13\times10^{-5}$). The reliable solutions with $\xi < 10^{-4}$ provide also for Taylor syntheses an accurate matching of the reference pattern with negligible errors confined to very low sidelobes, far from the mainlobe [see the inset of Fig. 4(d)], which do not contain relevant portions of the radiated power.

As for the element saving with respect to the $\lambda/2$-spaced arrangement, the values in Table I confirm that $P_{BCS}/P_{UNI} \in [0.65, 0.70]$ as well as the conclusion drawn for the Dolph-Chebyshev patterns on the distribution of the array elements (i.e., $1.43 \leq \Delta L/(\lambda/2) \leq 1.55$) and on the arising directivity ($D_{BCS}/D_{UNI} \in [0.995, 1.001]$—Table I). Concerning the computational issues, the BCS turns out to be very efficient ($t_{BCS} < 0.35$ [s]—Table I) whatever the broadside reference pattern, despite the non-optimized implementation of the Matlab code.

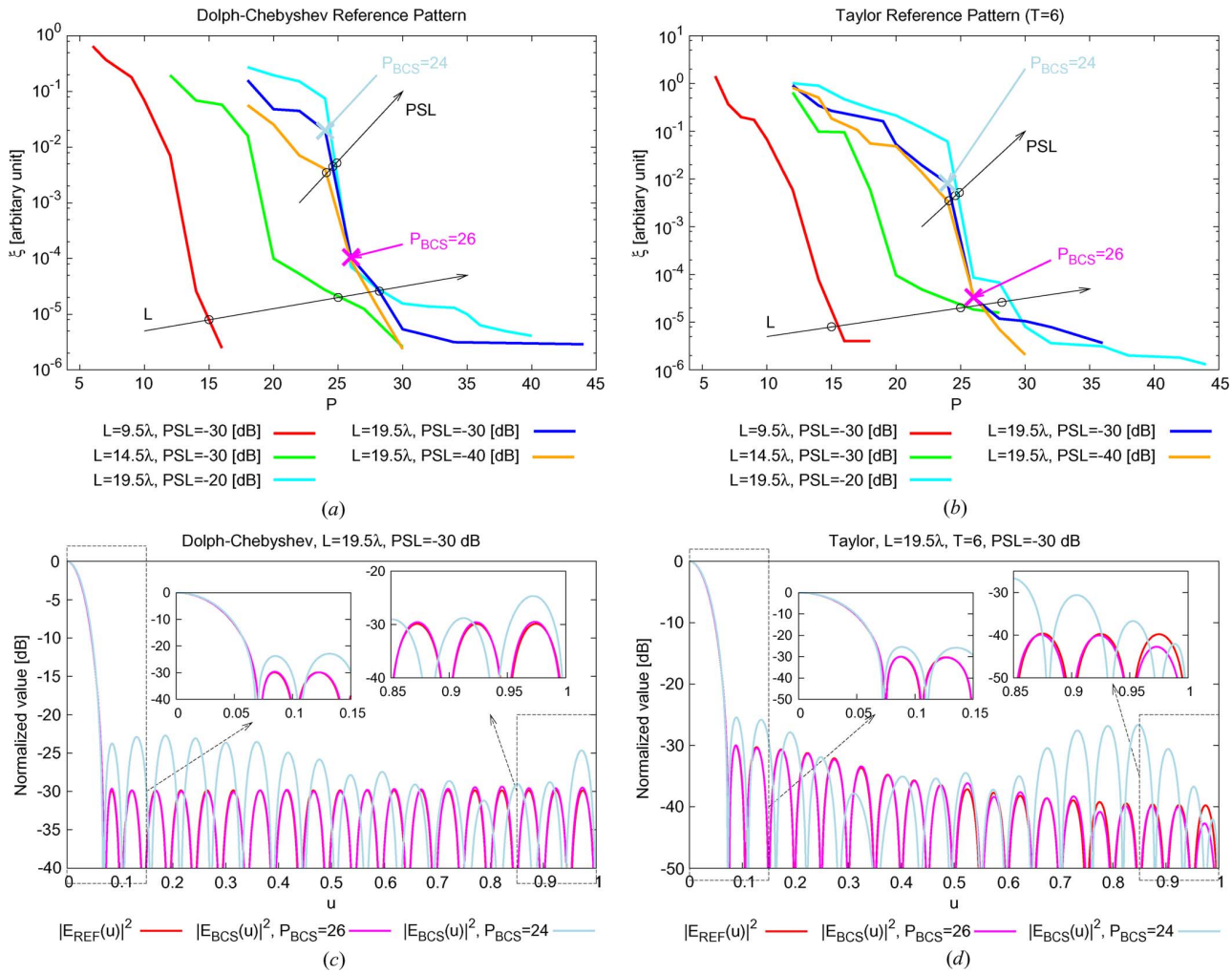

Fig. 4. *BCS Assessment* (*Broadside Pattern Synthesis*)—Pareto fronts in the (ξ, P_{BCS}) plane (*a*), (*b*) and power patterns (*c*), (*d*) of representative BCS solutions when matching (*a*), (*c*) Dolph-Chebyshev and (*b*), (*d*) Taylor reference patterns.

TABLE I
BCS Assessment (*Broadside Pattern Synthesis*)—ARRAY PERFORMANCE INDEXES

Reference Pattern			*Uniform*			*BCS*						
Type	L [λ]	PSL [dB]	P_{UNI}	$\frac{L_{UNI}}{L}$	D_{UNI} [dB]	ξ [$\times 10^{-5}$]	$\frac{P_{BCS}}{P_{UNI}}$	$\frac{\Delta L_{\min}}{\lambda/2}$	$\frac{\Delta L}{\lambda/2}$	$\frac{L_{BCS}}{L}$	D_{BCS} [dB]	t [$\times 10^{-1}$s]
Dolph	9.5	-30	20	1.0	12.39	2.62	0.70	1.26	1.46	1.000	12.39	1.12
Dolph	14.5	-30	30	1.0	14.19	9.98	0.66	1.35	1.52	1.000	14.19	2.93
Dolph	19.5	-20	40	1.0	15.44	7.10	0.65	1.50	1.56	0.997	15.42	2.14
Dolph	19.5	-30	40	1.0	15.44	3.03	0.70	0.78	1.42	0.995	15.43	1.18
Dolph	19.5	-40	40	1.0	14.93	9.09	0.65	1.56	1.56	1.000	14.92	1.13
Taylor	9.5	-30	20	1.0	12.34	7.82	0.70	1.22	1.46	1.000	12.32	1.27
Taylor	14.5	-30	30	1.0	14.10	9.64	0.66	1.35	1.52	1.000	14.11	3.14
Taylor	19.5	-20	40	1.0	15.87	8.53	0.65	1.34	1.55	0.994	15.86	1.92
Taylor	19.5	-30	40	1.0	15.35	3.13	0.65	0.80	1.43	0.993	15.34	1.48
Taylor	19.5	-40	40	1.0	14.86	3.62	0.65	1.36	1.54	0.990	14.85	1.01

In order to complete the analysis of the performance of the BCS approach when dealing with broadside patterns, comparisons with state-of-the-art techniques have been carried out, as well. Towards this purpose, the MPM approach [7][7] has been considered because of its efficiency and the enhanced matching accuracy compared to similar methods such as the Prony technique [7]. The results from the analysis of different Dolph-Chebyshev references are summarized in Fig. 5 where the plots of ξ versus P for both BCS and MPM[8] arrays are shown. Let us consider the test case characterized by a reference pattern with $PSL = -30$ [dB] defined over a linear aperture of length $L = 9.5\lambda$ [Fig. 5(a)]. In such

[7]A MATLAB implementation of the MPM has been used for the numerical tests (`mpencil` function—http://www.mathworks.se/matlabcentral/index.html) by setting the default parameters as suggested in [7].

[8]Please notice that only the MPM arrays with SVD-truncation parameter below 10^{-3} have been reported in order to guarantee an accurate pattern matching [7].

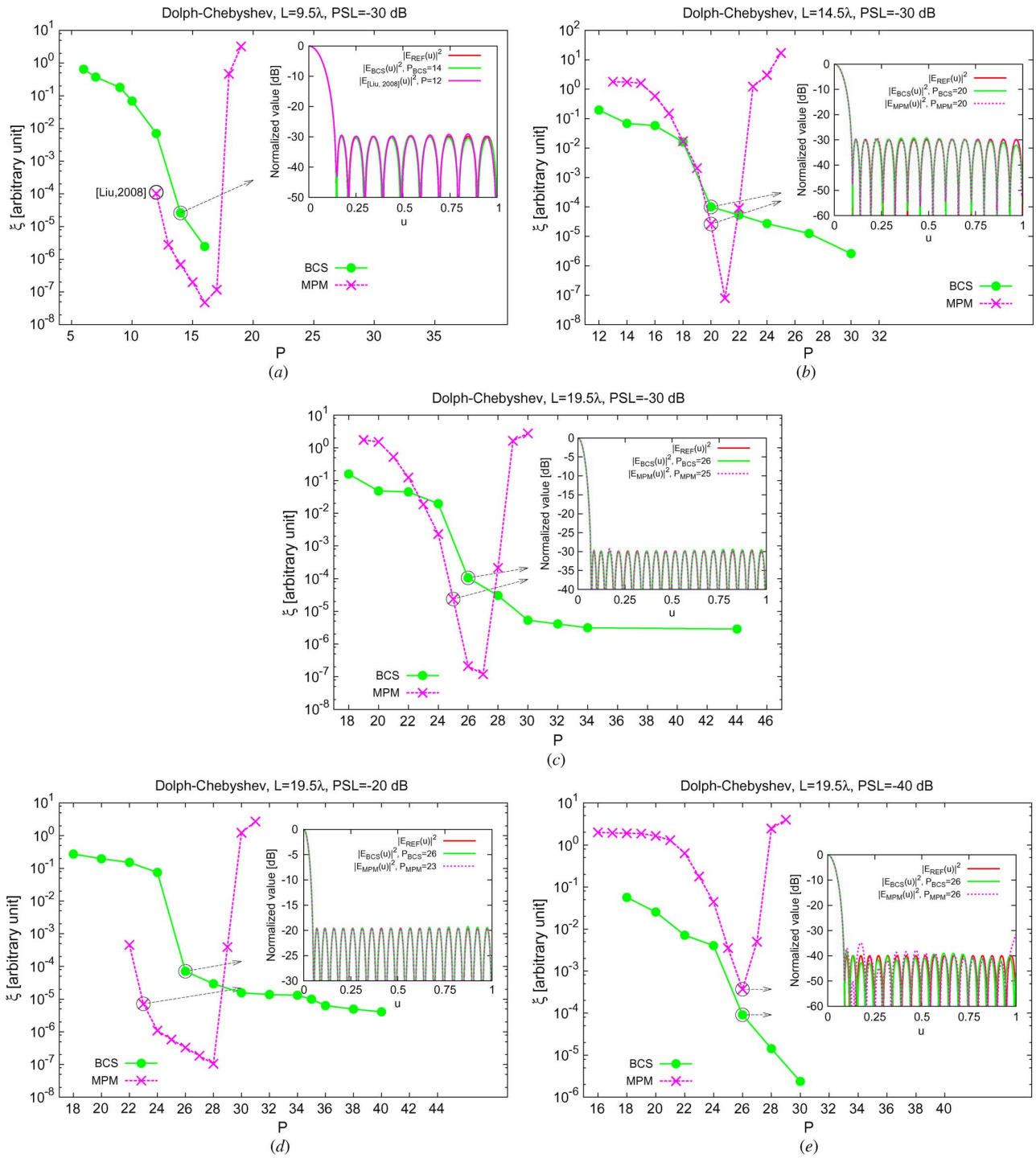

Fig. 5. BCS *Assessment* (*Broadside Pattern Synthesis*)—Representative points in the (ξ, P) plane of BCS and MPM solutions synthesized when matching the reference *Dolph-Chebyshev* patterns characterized by: (*a*) $L = 9.5\lambda - PSL = -30$ [dB], (*b*) $L = 14.5\lambda - PSL = -30$ [dB], (*c*) $L = 19.5\lambda - PSL = -30$ [dB], (*d*) $L = 19.5\lambda - PSL = -20$ [dB], and (*e*) $L = 19.5\lambda - PSL = -40$ [dB].

a case, the MPM provides a more accurate fitting than the BCS whatever the number of array elements (e.g., $P = 12 : \xi\rfloor_{BCS} = 7.02 \times 10^{-3}$ vs. $\xi\rfloor_{MPM} = 1.04 \times 10^{-4}$ [7]) and the BCS generally requires a larger P to satisfy the condition $\xi \leq 10^{-4}$ ($P_{BCS} = 14 \rightarrow \xi\rfloor_{BCS} = 2.62 \times 10^{-5}$ vs. $P_{MPM} = 13 \rightarrow \xi\rfloor_{BCS} = 2.76 \times 10^{-6}$). The BCS performances come closer to those of the MPM as L increases [$L = 14.5\lambda$—Fig. 5(b) and $L = 19.5\lambda$—Fig. 5(c)] and sometimes the BCS outperforms the MPM in terms of fitting index for both small and large values of P [Fig. 5(b) and (c)]. Moreover and with reference to Fig. 5(c)–(e), it results that the efficiency of the BCS enhances when PSL reduces. As a matter of fact, the MPM overcomes the BCS when $L = 19.5\lambda$ and $PSL = -20$ [dB] [Fig. 5(d)], while $\xi_{BCS} < \xi_{MPM}$ for the aperture $L = 19.5\lambda$ with $PSL = -40$ [dB] [Fig. 5(e)] as also pictorially pointed out by the plots of $E_{MPM}(u)$ and $E_{BCS}(u)$ synthesized with the corresponding $P = 26$-element arrangement [inset of

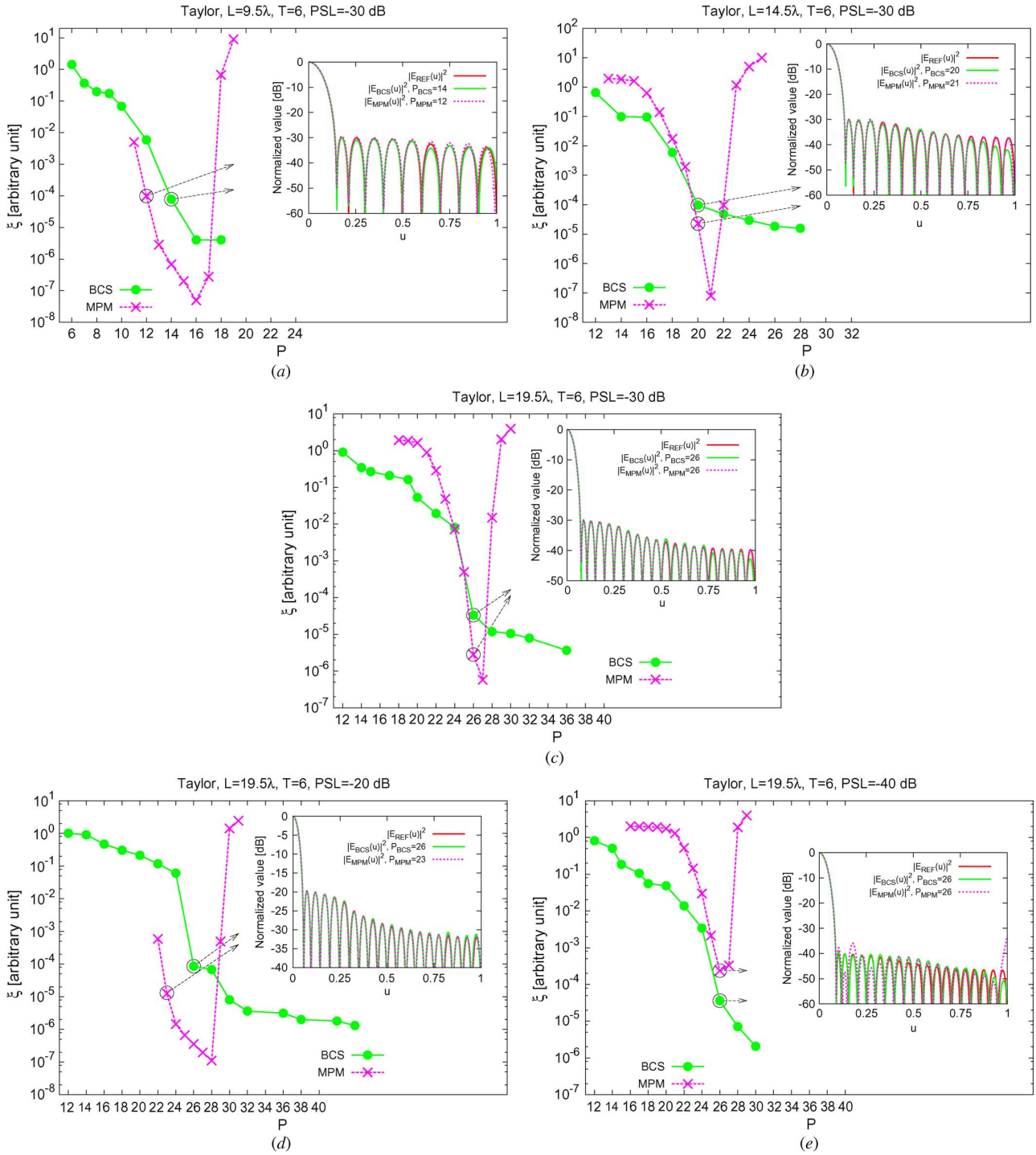

Fig. 6. *BCS Assessment* (*Broadside Pattern Synthesis*)—Representative points in the (ξ, P) plane of BCS and MPM solutions synthesized when matching the reference *Taylor* patterns characterized by: (*a*) $L = 9.5\lambda - PSL = -30$ [dB], (*b*) $L = 14.5\lambda - PSL = -30$ [dB], (*c*) $L = 19.5\lambda - PSL = -30$ [dB], (*d*) $L = 19.5\lambda - PSL = -20$ [dB], and (*e*) $L = 19.5\lambda, PSL = -40$ [dB].

Fig. 5(e)]. As it can be observed, the BCS properly matches the reference pattern within the entire visible range, while the MPM accuracy worsen near the mainlobe and in the far sidelobes.

Similar conclusions hold true when dealing with Taylor reference patterns. The behavior of ξ versus P (Fig. 6) still indicates that the MPM outperforms the BCS concerning the minimum P to reach the matching threshold $\xi = 10^{-4}$ when dealing with small arrays and high PSLs [$P_{MPM} = 12 \rightarrow \xi_{MPM} = 9.89 \times 10^{-5}$ vs. $P_{BCS} = 14 \rightarrow \xi_{BCS} = 7.82 \times 10^{-5}$—Fig. 6(a)], while the BCS betters the MPM performance for larger L with low peak sidelobe levels [$P_{MPM} = 26 \rightarrow \xi_{MPM} = 2.38 \times 10^{-4}$ vs. $P_{BCS} = 26 \rightarrow \xi_{BCS} = 3.62 \times 10^{-5}$—Fig. 6(e)]. This is further confirmed by the patterns of the optimal trade-off solutions displayed in the insets of the pictures of Fig. 6.

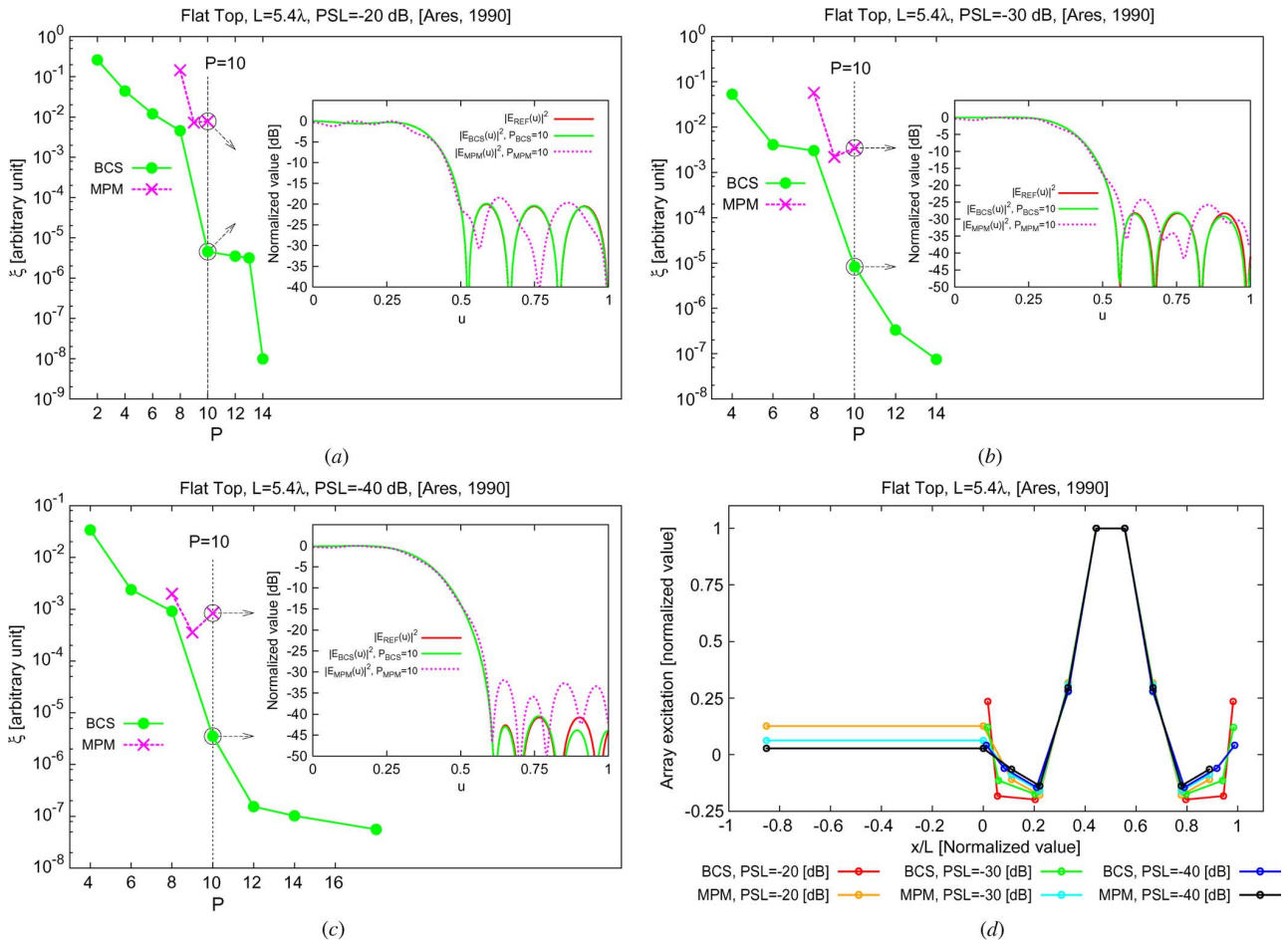

Fig. 7. BCS *Assessment* (*Shaped Pattern Synthesis*: $L = 5.4\lambda$ [38])—Representative points in the (ξ, P) plane of BCS and MPM solutions synthesized when matching the reference *Shaped* patterns [38] characterized by: (*a*) $PSL = -20$ dB, (*b*) $PSL = -30$ [dB], and (*c*) $PSL = -40$ [dB]. Array excitations (*d*).

TABLE II
BCS *Assessment* (*Shaped Pattern Synthesis*: $L = 5.4\lambda$ [38])—ARRAY PERFORMANCE INDEXES

Reference Pattern		*Method*	*Indexes*						
L [λ]	PSL [dB]		ξ	P	$\frac{\Delta L_{\min}}{\Delta L_{UNI}}$	$\frac{\Delta L}{\Delta L_{UNI}}$	$\frac{L}{L_{UNI}}$	D [dB]	t [s]
5.4	-20	[38]	–	10	1.00	1.00	1.00	4.40	–
5.4	-20	BCS	4.55×10^{-6}	10	0.34	0.96	0.96	4.40	1.5×10^{-1}
5.4	-20	MPM	7.82×10^{-3}	10	0.99	1.74	1.74	4.68	3.3×10^{-2}
5.4	-30	[38]	–	10	1.00	1.00	1.00	4.30	–
5.4	-30	BCS	8.27×10^{-6}	10	0.39	0.96	0.96	4.29	1.4×10^{-1}
5.4	-30	MPM	3.45×10^{-3}	10	0.99	1.74	1.74	4.66	2.5×10^{-2}
5.4	-40	[38]	–	10	1.00	1.00	1.00	4.45	–
5.4	-40	BCS	3.53×10^{-6}	10	0.63	0.97	0.97	4.45	1.6×10^{-1}
5.4	-40	MPM	0.84×10^{-3}	10	0.99	1.74	1.74	4.63	2.9×10^{-2}

C. BCS Assessment—Synthesis of Shaped Patterns

In order to evaluate the flexibility of the proposed approach, numerical tests concerned with shaped patterns have been also performed. The first experiment deals with the reconstruction of flat top patterns defined over an aperture of $L = 4.5\lambda$ with different PSLs as in [38]. The plots of ξ as a function of P show that neither the MPM nor the BCS is able to reduce the number of array elements of the uniform array (being 0.6λ its inter-element distance) synthesized in [38] still keeping a good accuracy, although the BCS [$P_{BCS} = 10 \rightarrow \xi_{BCS} = 4.55 \times 10^{-6}$—Fig. 7(a)] reduces the array aperture with respect to [38] ($L_{BCS}/L < 0.97$—Table II). On the contrary, the MPM defines wider arrangements ($L_{MPM}/L = 1.74$), as shown in Fig. 7(d), without yielding a good matching with the reference patterns ($\xi_{MPM} > 2.5 \times 10^{-3}$—Table II). The enhanced accuracy of the BCS is also pointed out by the plots of $E_{REF}(u)$, $E_{BCS}(u)$, and $E_{MPM}(u)$ in the insets of Figs. 7(a)–7(c) related to the arrays with $P_{BCS} = P_{MPM} = 10$. For completeness, the distributions of the array excitations

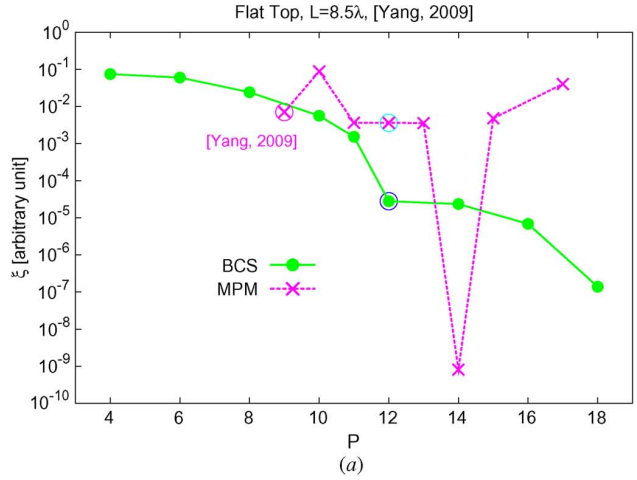

Fig. 8. *BCS Assessment* (*Flat-Top Pattern Synthesis*: $L = 8.5\lambda$ [39])—Representative points in the (ξ, P) plane of BCS and MPM solutions (*a*), optimal trade-off beampatterns (*b*), and associated array excitations (*c*).

along the array extension are given in Fig. 7(d). As it can be observed and also predicted in [7], the worsening of the performances of the MPM is mainly due to the errors in estimating the element positions caused by the non-negligible values of the imaginary parts of the non-zero roots of the associated eigenvalue problem.

The second experiment considers as reference the *Woodward* pattern with $L = 8.5\lambda$ analyzed in [39]. The plots of

TABLE III
BCS Assessment (*Shaped Pattern Synthesis*: $L = 8.5\lambda$ [39])—ARRAY PERFORMANCE INDEXES

	Uniform	*BCS*	*MPM*	*MPM* [39]
L [λ]	8.5	8.33	8.36	8.50
PSL [dB]	-20	-20.2	-13.2	-14.63
P	18	12	12	9
$\frac{P}{P_{UNI}}$	–	0.66	0.66	0.50
$\frac{\Delta L_{\min}}{\Delta L_{UNI}}$	–	1.18	< 0.01	1.42
$\frac{\Delta L}{\Delta L_{UNI}}$	–	1.51	1.52	2.12
$\frac{L}{L_{UNI}}$	–	0.980	0.984	1.00
t [s]	–	2.0×10^{-1}	2.8×10^{-1}	–
ξ	–	2.79×10^{-5}	4.02×10^{-3}	7.02×10^{-3}
D [dB]	6.21	6.22	6.18	6.34

ξ versus P show that the BCS faithfully reconstructs the reference pattern synthesizing an array of $P_{BCS} = 12$ elements [$\xi_{BCS} = 2.79 \times 10^{-5}$—Fig. 8(a)] with a reduction of about 1/3 of the array elements with respect to the uniform layout ($P_{UNI} = 18$). As a side effect of the approximation, the optimal BCS trade-off slightly improves the PSL of the reference pattern ($P_{BCS} = 12 \rightarrow PSL_{BCS} = -20.2$ [dB] vs. $PSL_{UNI} = -20$ [dB]—Table III), as well. On the contrary, both the MPM synthesis in [39] and the MPM pattern generated with $P_{MPM} = 12$ elements do not provide an accurate fitting [$P_{MPM} = 12 \rightarrow \xi_{MPM} = 4.02 \times 10^{-3}$—Fig. 8(a)], unless using more antenna elements (e.g., $P_{MPM} = 14$), and significantly worsen the PSL ($P_{MPM} = 12 \rightarrow PSL_{MPM} = -13.2$ [dB]) as highlighted by the plots of the associated patterns [Fig. 8(b)]. For completeness, the behaviour of the array excitations and the corresponding figures of merit are reported in Fig. 8(c) and Table III, respectively. As for the computational costs, the BCS still retains the numerical efficiency proved in synthesizing broadside patterns (Table III).

Similar conclusions can be also drawn when considering wider reference apertures. For example, with reference to a Woodward reference pattern with $L = 19.5\lambda$ [Fig. 9(a)], the BCS yields an accurate approximation with less elements than the MPM ($P_{BCS} = 26$ vs. $P_{MPM} = 28$). Moreover, the accuracy of the MPM significantly worsens when using the same number of active elements of the BCS solution [$P = 26 - \xi_{MPM} = 4.81 \times 10^{-2}$, $PSL_{MPM} = -3.6$ [dB] vs. $\xi_{BCS} = 3.52 \times 10^{-5}$, $PSL_{BCS} = -17.4$—Table IV and Fig. 9(b)]. As for the array arrangement, the BCS provides a more widely-spaced design characterized by the following parameters: $\Delta L_{\min}/\lambda/2 = 0.975$ and $\Delta L/\lambda/2 = 1.56$ (Table IV).

D. *BCS Assessment—Constrained Synthesis*

This section is devoted to assess the reliability of the BCS approach in solving constrained synthesis problems (i.e., matching a reference pattern under some explicit geometric and/or radiation constraints). Towards this aim, the synthesis of a Dolph-Chebyshev pattern with $L = 19.5\lambda$ and $PSL = -30$ [dB] under different synthesis constraints has been addressed. The first test case has been formulated by enforcing the pattern matching constraints in the angular

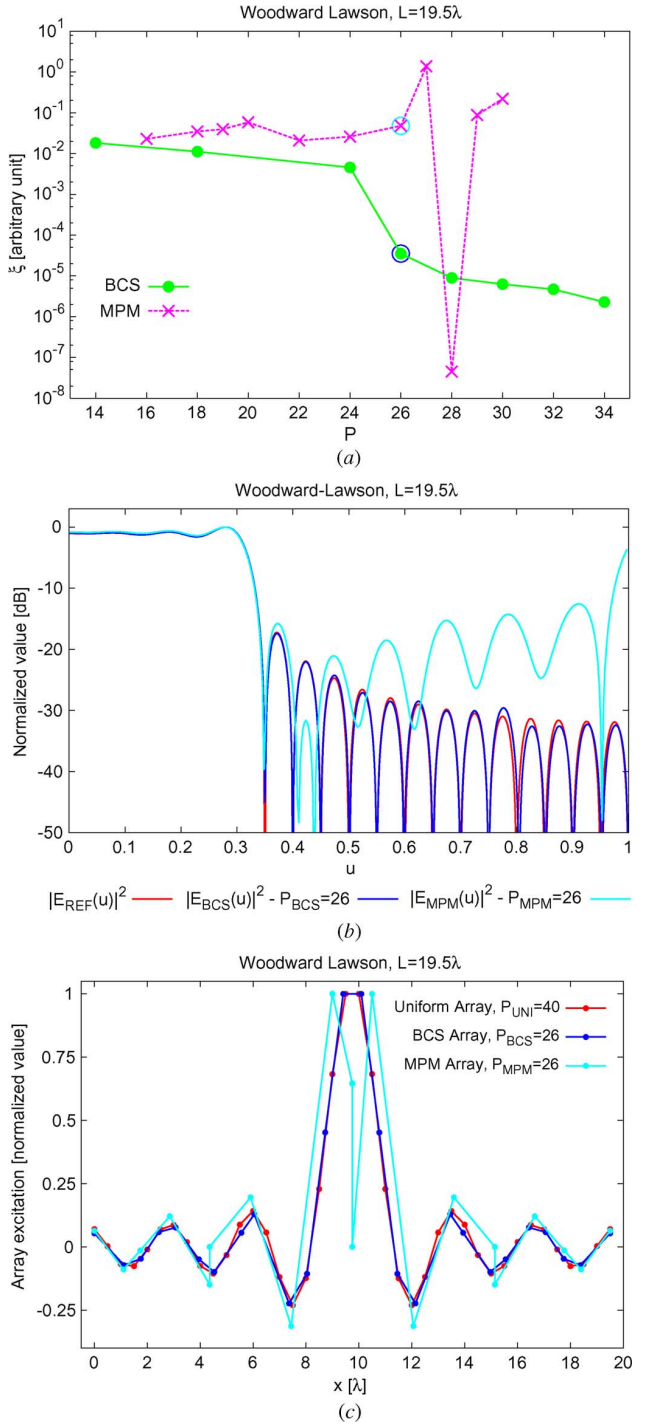

Fig. 9. BCS *Assessment* (*Flat Top Pattern Synthesis*: $L = 19.5\lambda$)— Representative points in the (ξ, P) plane of BCS and MPM solutions (*a*), optimal trade-off beampatterns (*b*), and associated array excitations (*c*).

TABLE IV
BCS *Assessment* (*Shaped Pattern Synthesis*: $L = 19.5\lambda$)—Array Performance Indexes

	Uniform (WLM)	BCS	MPM
L [λ]	19.5	19.5	19.5
PSL [dB]	-17.2	-17.4	-3.6
P	40	26	26
$\frac{P}{P_{UNI}}$	–	0.65	0.65
$\frac{\Delta L_{\min}}{\Delta L_{UNI}}$	–	0.975	< 0.01
$\frac{\Delta L}{\Delta L_{UNI}}$	–	1.56	1.56
$\frac{L}{L_{UNI}}$	–	1.0	1.0
t [s]	–	1.4×10^{-1}	3.3×10^{-1}
ξ		3.52×10^{-5}	4.81×10^{-2}
D [dB]	5.91	5.92	5.91

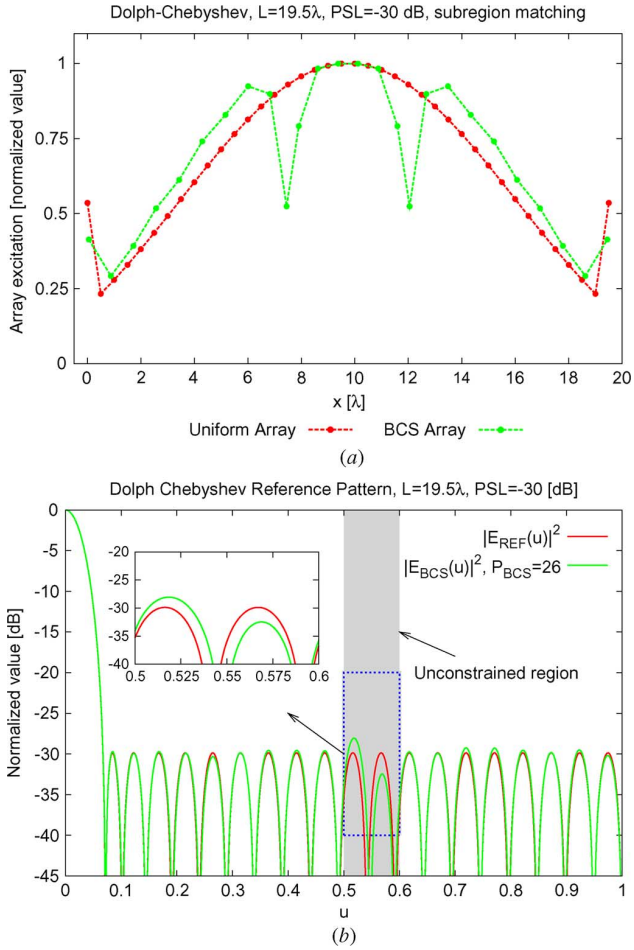

Fig. 10. BCS *Assessment* [*Constrained Synthesis—Dolph-Chebyshev*: $L = 19.5\lambda, u_k \notin (0.45, 0.55)$]—Array excitations (*a*) and power patterns (*b*).

region $u_k \notin [u_m, u_M]$, being $u_m = 0.5$ and $u_M = 0.6$. As desired, the pattern of the optimal BCS trade-off solution ($\xi = 3.71 \times 10^{-5}$—Table V) fits in a faithful way the reference one within the constrained region as well as in the transition regions close to the unconstrained angular range [Fig. 10(b)]. It is also of interest to observe that the distribution of the array excitations of the BCS synthesis and those of the uniform array quite significantly differ [Fig. 10(a)].

To further verify the efficiency of the BCS to include pattern constraints in the synthesis process without affecting the reliability of the matching in the remaining portion of the pattern, the constraint has been moved in another region of the visible range by setting $u_m = 0.8$ and $u_M = 1.0$. As expected, the trade-off pattern carefully matches the reference in the constrained region ($\xi = 6.81 \times 10^{-5}$—Table V), while uncontrolled lobes appear for $u > 0.8$ [Fig. 11(b)]. The use of a directive element [e.g., a

TABLE V
BCS Assessment (*Constrained Synthesis—Dolph-Chebyshev*: $L = 19.5\lambda$)—ARRAY PERFORMANCE INDEXES

Reference Pattern		*Constraint*	*BCS Indexes*						
L [λ]	PSL [dB]		ξ	P	$\Delta L_{min}[\lambda]$	ΔL [λ]	L [λ]	D [dB]	t [$\times 10^{-1}$s]
19.5	-30	$u_k \notin (0.5, 0.6)$	3.71×10^{-5}	26	0.455	0.776	19.36	15.43	2.17
19.5	-30	$u_k \notin (0.8, 1)$	6.81×10^{-5}	21	0.585	0.928	19.50	14.34	1.40
19.5	-30	$d_n \notin (5.3, 6.5)$ [λ]	5.82×10^{-6}	36	0.067	0.556	19.47	15.44	1.61
19.5	-30	$d_n \notin (0, 1)$ [λ]	4.81×10^{-5}	30	0.029	0.670	19.44	15.43	1.65

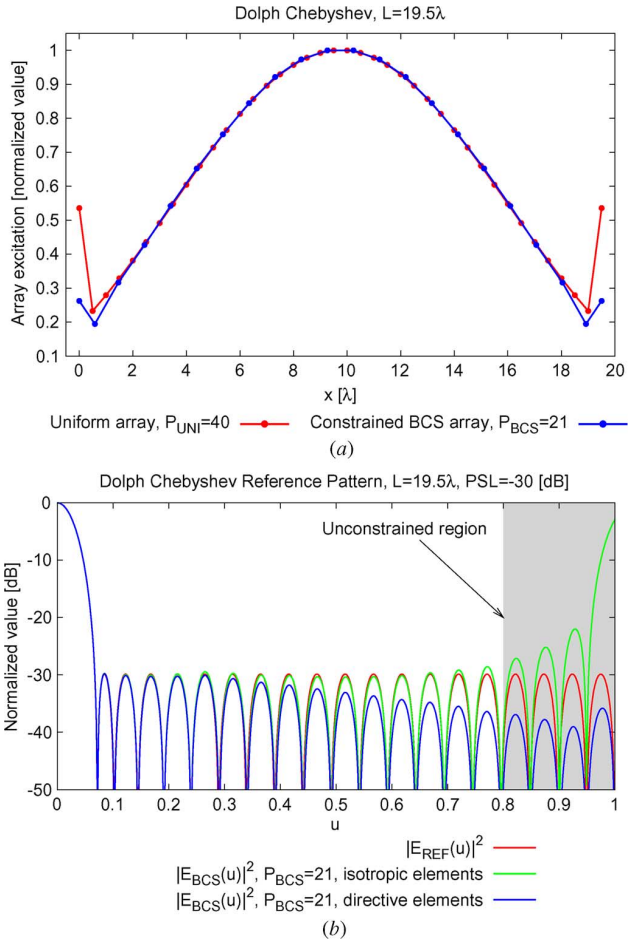

Fig. 11. *BCS Assessment* (*Constrained Synthesis—Dolph-Chebyshev*: $L = 19.5\lambda, u_k \notin (0.8, 1.0]$)—Array excitations (*a*) and power patterns when using isotropic or directive elements (*b*).

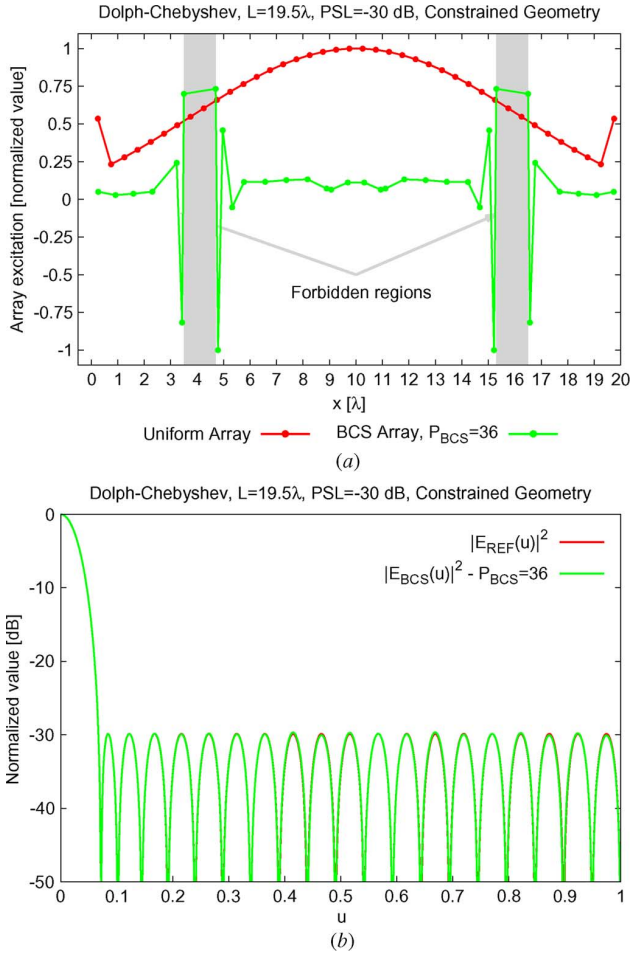

Fig. 12. *BCS Assessment* [*Constrained Synthesis—Dolph-Chebyshev*: $L = 19.5\lambda, d_n \notin (5.3\lambda, 6.5\lambda)$]—Array excitations (*a*) and power patterns (*b*).

$cos(\theta)$ radiating element] might then enable the control of the sidelobes in the whole visible region [Fig. 11(b)] with a significant saving of active elements in comparison with the uniform array synthesizing the entire Dolph pattern ($P_{BCS} = 21$ vs. $P_{UNI} = 40$).

The last part of the numerical assessment is aimed at analyzing the capability of the BCS approach to also take into account geometrical constraints. Towards this end and considering the same reference pattern of the previous experiments, two different aperture-blockage problems have been defined: (*i*) $d_n \notin [5.3\lambda, 6.5\lambda]$ and (*ii*) $d_n \notin [0.0\lambda, 1.0\lambda]$. The plots of the synthesized trade-off arrangements assess the effectiveness and reliability of the BCS technique in constraining the element positions to desired locations [Figs. 12(a) and 13(a)], while designing sparse arrangements ($\Delta L > \lambda/2$—Table V) with reduced apertures ($L_{BCS} < 19.47$), as well. It is also worthwhile to point out that, notwithstanding the non-negligible reduction of the admissible spatial region for the array elements (more than 10% in both cases), the $E_{BCS}(u)$ pattern matches the reference $E_{REF}(u)$ with a great care [Fig. 12(b) and Fig. 13(b)] as confirmed by the values of the matching index [(*i*) $\xi = 5.82 \times 10^{-6}$ and (*ii*) $\xi = 4.81 \times 10^{-5}$—Table V].

V. CONCLUSIONS

In this paper, the BCS has been proposed as an innovative, flexible, and computationally-efficient complement to the existing state-of-the-art methods for the synthesis of sparse arrays with desired radiation properties. The pattern matching problem

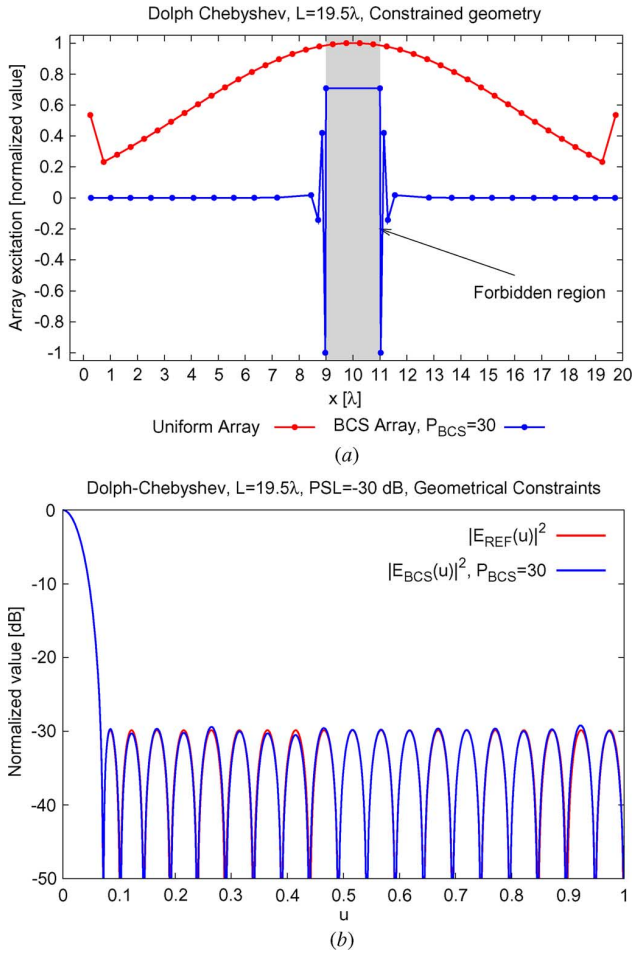

Fig. 13. *BCS Assessment* [*Constrained Synthesis—Dolph-Chebyshev*: $L = 19.5\lambda$, $d_n \notin (0.0\lambda, 1.0\lambda)$]—Array excitations (*a*) and power patterns (*b*).

has been properly reformulated in a suitable Bayesian framework and successively solved with a fast solver. An extensive numerical validation has been carried out dealing with different reference patterns, array sizes, and constraints to assess the feasibility and reliability of the BCS approach as well as its efficiency, flexibility, and accuracy. Selected comparisons with state-of-the-art techniques have highlighted the advantages and (in some special cases) limitations of the BCS synthesis in terms of sensitivity on control parameters, performances, and computational complexity. The proposed technique has shown the following main features:

- several tradeoffs solutions can be easily obtained by means of simple modifications of the control parameters (σ^2, u_k, d_n, and σ_0^2) (Section III-A);
- BCS favorably compares with state-of-the-art techniques such as the MPM [7] in terms of accuracy, array sparseness, and computational burden when matching reference broadside patterns (Section III-B);
- on average the number of active elements in a BCS array turns out to be smaller than the corresponding uniform arrangement ($P_{BCS} \approx 0.7 \div 0.65\ P_{UNI}$) still providing a high accuracy in matching the reference pattern (i.e., $\xi \leq 10^{-4}$);
- despite no specific constraints (e.g., on the maximum percentage of antenna elements that can be thinned) have been enforced and unlike previous array thinning techniques, the directivity of BCS sparse arrays is very close to that of their fully-populated counterparts (Table I–IV);
- BCS usually outperforms MPM when dealing with shaped beampatterns (Section III-C);
- application-specific constraints on either the radiation pattern or the geometrical characteristics of the array can be easily and efficiently taken into account (Section III-D).

Subjects of future researches will be the analysis of the mutual coupling effects in the presence of realistic array elements as well as an enhanced exploitation of directive elements. Further extensions, out-of-the-scope of the present paper, will concern with complex excitations and non-symmetric layouts. Moreover, further works will be done on the sensitivity on control parameters, performances and on the reduction of the computational complexity of the method.

APPENDIX

Sequential Solver for the Maximization of $\mathcal{L}(\mathbf{a}, \sigma^2)$: The marginal likelihood maximization algorithm proposed in [35] is hereinafter customized to deal with user-defined pattern matching problems. Starting from the knowledge of $\mathbf{E}_{REF}$ and Ψ, the following sequence is iteratively (r being the iteration index) applied:

1) **Initialization** $(r = 0)$—Set $[\sigma^2]^{(r)} = var[\mathbf{E}_{REF}] \times \sigma_0^2$ and the n-th entry of the diagonal matrix $A^{(r)} \triangleq diag(a_1^{(r)}, \ldots, a_N^{(r)})$ as follows
$$a_n^{(r)} = \frac{||\psi_n||^4}{||\psi_n^T \mathbf{E}_{REF}||^2 - [\sigma^2]^{(r)}||\psi_n||^2} \tag{17}$$
if $n = \hat{n}$ and $a_n^{(r)} = \infty$ otherwise, $\hat{n}$ and ψ_n being randomly picked integers within $[1, N]$ and the n-th column of Ψ, respectively;
2) **Update**—Evaluate $\Sigma^{(r)} = \Sigma(A^{(r)}, [\sigma^2]^{(r)})$ and $\mu^{(r)} = \mu(A^{(r)}, [\sigma^2]^{(r)})$ to compute the *sparsity* factors $s_n^{(r)} = \psi_n^T C_{-n}^{-1} \psi_n$, $n = 1, \ldots, N$ and the *quality* factors $z_n^{(r)} = \psi_n^T C_{-n}^{-1} \mathbf{E}_{REF}$, $n = 1, \ldots, N$ where $C_{-n} = C - a_n^{-1} \psi_n \psi_n^T$;
3) **Candidate Basis Vector Evaluation**—Select the r-th candidate basis vector[9] ψ_n, $n = r$, and compute $\Theta_n^{(r)} = (z_n^{(r)})^2 - s_n^{(r)}$. If $\Theta_n^{(r)} > 0$, then update the value of $a_n^{(r)}$ by means of (17), otherwise set $a_n^{(r)} = \infty$;
4) **Convergence Check**—Compute the value of $\Theta_n^{(r)} \forall n \in 1, \ldots, N$. If $\Theta_n^{(r)} \leq \tau \forall n$ (τ being the *tolerance factor* usually set to 10^{-8} [37]), then terminate. Otherwise, update the iteration index $(r \leftarrow r + 1)$ and go to step 2.

ACKNOWLEDGMENT

The authors wish to thank Dr. S. Ji, Dr. Y. Xue, and Prof. L. Carin for sharing the BCS code online.

[9]Please refer to [35] for a review of the strategies for candidate selection.

REFERENCES

[1] C. A. Balanis, *Antenna Theory: Analysis and Design*, 2nd ed. New York: Wiley, 1997.

[2] R. J. Mailloux, *Phased Array Antenna Handbook*, 2nd ed. Norwood, MA: Artech House, 2005.

[3] R. M. Leahy and B. D. Jeffs, "On the design of maximally sparse beamforming arrays," *IEEE Trans. Antennas Propag.*, vol. 39, no. 8, pp. 1178–1187, Aug. 1991.

[4] D. King, R. Packard, and R. Thomas, "Unequally spaced, broadband antenna arrays," *IRE Trans. Antennas Propag.*, vol. AP-8, pp. 380–384, Jul. 1960.

[5] A. Maffett, "Array factors with nonuniform spacing arrays," *IRE Trans. Antennas Propag.*, vol. AP-10, pp. 131–136, Mar. 1962.

[6] N. Balakrishan, P. Murthy, and S. Ramakrishna, "Synthesis of antenna arrays with spatial and excitation constraints," *IEEE Trans. Antennas Propag.*, vol. AP-29, pp. 690–696, Sep. 1962.

[7] Y. Liu, Z. Nie, and Q. H. Liu, "Reducing the number of antenna elements in a linear antenna array by the matrix pencil method," *IEEE Trans. Antennas Propag.*, vol. 56, no. 9, pp. 2955–2962, Sep. 2008.

[8] R. F. Harrington, "Sidelobe reduction by nonuniform element spacing," *IEEE Trans. Antennas Propag.*, vol. AP-9, p. 187, Mar. 1961.

[9] M. G. Andreasan, "Linear arrays with variable interelement spacings," *IEEE Trans. Antennas Propag.*, vol. AP-10, pp. 137–143, Mar. 1962.

[10] A. Ishimaru, "Theory of unequally-spaced arrays," *IEEE Trans. Antennas Propag.*, vol. AP-11, pp. 691–702, Nov. 1962.

[11] Y. T. Lo, "A mathematical theory of antenna arrays with randomly spaced elements," *IEEE Trans. Antennas Propag.*, vol. 12, no. 3, pp. 257–268, May 1964.

[12] M. I. Skolnik, G. Nemhauser, and J. W. Sherman, "Dynamic programming applied to unequally-space arrays," *IRE Trans. Antennas Propagat.*, vol. AP-12, pp. 35–43, Jan. 1964.

[13] J. Perini and M. Idselis, "Note on antenna pattern synthesis using numerical iterative methods," *IEEE Trans. Antennas Propag.*, vol. 19, no. 2, pp. 284–286, Mar. 1971.

[14] R. W. Redlich, "Iterative least-squares of nonuniformly spaced linear arrays," *IEEE Trans. Antennas Propag.*, vol. AP-21, no. 1, pp. 106–108, Jan. 1973.

[15] B. Steinberg, "The peak sidelobe of the phased array having randomly located elements," *IEEE Trans. Antennas Propag.*, vol. 20, no. 2, pp. 129–136, Mar. 1972.

[16] P. Jarske, T. Sramaki, S. K. Mitra, and Y. Neuvo, "On the properties and design of nonuniformly spaced linear arrays," *IEEE Trans. Acoust., Speech, Signal Processing*, vol. 36, pp. 372–380, Mar. 1988.

[17] R. L. Haupt, "Thinned arrays using genetic algorithms," *IEEE Trans. Antennas Propag.*, vol. 42, no. 7, pp. 993–999, Jul. 1994.

[18] V. Murino, A. Trucco, and C. S. Regazzoni, "Synthesis of unequally spaced arrays by simulated annealing," *IEEE Trans. Signal Processing*, vol. 44, no. 1, pp. 119–123, Jan. 1996.

[19] S. Holm, B. Elgetun, and G. Dahl, "Properties of the beampattern of weight- and layout-optimized sparse arrays," *IEEE Trans. Ultrason., Ferroelectr., Freq. Control*, vol. 44, no. 5, pp. 983–991, Sep. 1997.

[20] A. Trucco and V. Murino, "Stochastic optimization of linear sparse arrays," *IEEE J. Ocean. Engrg.*, vol. 24, no. 3, pp. 291–299, Jul. 1999.

[21] B. P. Kumar and G. R. Branner, "Design of unequally spaced arrays for performance improvement," *IEEE Trans. Antennas Propag.*, vol. 47, pp. 511–523, Mar. 1999.

[22] D. G. Leeper, "Isophoric arrays—Massively thinned phased arrays with well-controlled sidelobes," *IEEE Trans. Antennas Propag.*, vol. 47, no. 12, pp. 1825–1835, Dec. 1999.

[23] F. B. T. Marchaud, G. D. de Villiers, and E. R. Pike, "Element positioning for linear arrays using generalized Gaussian quadrature," *IEEE Trans. Antennas Propag.*, vol. 51, no. 6, pp. 1357–1363, Jun. 2003.

[24] D. G. Kurup, M. Himdi, and A. Rydberg, "Synthesis of uniform amplitude unequally spaced antenna array using the differential evolution algorithm," *IEEE Trans. Antennas Propag.*, vol. 51, pp. 2210–2217, Sep. 2003.

[25] S. Caorsi, A. Lommi, A. Massa, and M. Pastorino, "Peak sidelobe reduction with a hybrid approach based on GAs and difference sets," *IEEE Trans. Antennas Propag.*, vol. 52, no. 4, pp. 1116–1121, Apr. 2004.

[26] B. P. Kumar and G. R. Branner, "Generalized analytical technique for the synthesis of unequally spaced arrays with linear, planar, cylindrical or spherical geometry," *IEEE Trans. Antennas Propag.*, vol. 53, pp. 621–633, Feb. 2005.

[27] T. G. Spence and D. H. Werner, "Thinning of aperiodic antenna arrays for low side-lobe levels and broadband operation using genetic algorithms," in *Proc. IEEE Antennas Propag. Society Int. Symp.*, Jul. 9–14, 2006, pp. 2059–2062.

[28] T. G. Spence and D. H. Werner, "Design of broadband planar arrays based on the optimization of aperiodic tilings," *IEEE Trans. Antennas Propag.*, vol. 56, no. 1, pp. 76–86, Jan. 2008.

[29] R. L. Haupt and D. H. Werner, *Genetic Algorithms in Electromagnetics*. Hoboken, NJ: Wiley, 2007.

[30] P. J. Bevelacqua and C. A. Balanis, "Minimum sidelobe levels for linear arrays," *IEEE Trans. Antennas Propag.*, vol. 55, pp. 2210–2217, Dec. 2007.

[31] G. Oliveri, M. Donelli, and A. Massa, "Linear array thinning exploiting almost difference sets," *IEEE Trans. Antennas Propag.*, vol. 57, no. 12, pp. 3800–3812, Dec. 2009.

[32] S. Ji, Y. Xue, and L. Carin, "Bayesian compressive sensing," *IEEE Trans. Signal Process.*, vol. 56, no. 6, pp. 2346–2356, Jun. 2008.

[33] M. E. Tipping, "Sparse bayesian learning and the relevance vector machine," *J. Machine Learning Res.*, vol. 1, pp. 211–244, 2001.

[34] A. C. Faul and M. E. Tipping, "Analysis of sparse Bayesian learning," in *Advances in Neural Information Processing Systems (NIPS 14)*, T. G. Dietterich, S. Becker, and Z. Ghahramani, Eds., 2002, pp. 383–389 [Online]. Available: http://citeseer.ist.psu.edu/faul01analysis.html

[35] M. E. Tipping and A. C. Faul, "Fast marginal likelihood maximization for sparse Bayesian models," in *Proc. 9th Int. Workshop Artificial Intelligence and Statistics*, C. M. Bishop and B. J. Frey, Eds., 2003 [Online]. Available: http://citeseer.ist.psu.edu/611465.html

[36] M. E. Tipping, "The relevance vector machine," in *Advances in Neural Information Processing Systems*, S. A. Solla, T. K. Leen, and K.-R. Muller, Eds. Cambridge, MA: MIT Press, 2000, vol. 12, pp. 652–658.

[37] S. Ji, Y. Xue, and L. Carin, Bayesian Compressive Sensing Code 2009 [Online]. Available: http://people.ee.duke.edu/~lihan/cs/

[38] F. Ares and E. Moreno, "The convolution applied on the synthesis shaped beam," in *Proc. 20th Eur. Microwave Conf.*, Oct. 1990, vol. 2, pp. 1491–1494.

[39] S. Yang, Y. Liu, and Q. H. Liu, "Combined strategies based on matrix pencil method and tabu search algorithm to minimize elements of non-uniform antenna array," *Progr. Electromagn. Res. B*, vol. 18, pp. 259–277, 2009.

Giacomo Oliveri (M'10) received the B.S. and M.S. degrees in telecommunications engineering and the Ph.D. degree in space sciences and engineering from the University of Genoa, Italy, in 2003, 2005, and 2009 respectively.

Since 2008, he has been a member of the Electromagnetic Diagnostic Laboratory, University of Trento, Italy. His research work is mainly focused on cognitive radio systems, electromagnetic direct and inverse problems, and antenna array design and synthesis.

Andrea Massa (M'96) received the "Laurea" degree in electronic engineering and Ph.D. degree in electronics and computer science from the University of Genoa, Genoa, Italy, in 1992 and 1996, respectively.

From 1997 to 1999, he was an Assistant Professor of electromagnetic fields in the Department of Biophysical and Electronic Engineering, University of Genoa, teaching the university course, Electromagnetic Fields 1. From 2001 to 2004, he was an Associate Professor at the University of Trento, Trento, Italy, where, since 2005, he has been a Full Professor teaching electromagnetic fields, inverse scattering techniques, antennas and wireless communications, and optimization techniques. He is also the Director of the ELEDIALab at the University of Trento and Deputy Dean of the Faculty of Engineering. Since 1992, his research has focused on electromagnetic direct and inverse scattering, microwave imaging, optimization techniques, wave propagation in presence of nonlinear media, wireless communications and applications of electromagnetic fields to telecommunications, medicine and biology.

Prof. Massa is a member of the IEEE Society, the PIERS Technical Committee, and the Inter-University Research Center for Interactions Between Electromagnetic Fields and Biological Systems (ICEmB). He is the Italian representative in the general assembly of the European Microwave Association (EuMA).